Available online at www.sciencedirect.com
ScienceDirect
Trans. Nonferrous Met. Soc. China 30(2020) 200−211
Transactions of Nonferrous Metals Society of China
www.tnmsc.cn

Photogenerated-hole scavenger for enhancing photocatalytic chalcopyrite bioleaching

Bao-jun YANG[1,2], Wen LUO[3], Qi LIAO[4], Jian-yu ZHU[1,2,4], Min GAN[1,2], Xue-duan LIU[1,2], Guan-zhou QIU[1,2]

1. School of Minerals Processing and Bioengineering, Central South University, Changsha 410083, China;
2. Key Laboratory of Biohydrometallurgy of Ministry of Education, Central South University, Changsha 410083, China;
3. The Second Xiangya Hospital of Central South University, Changsha 410011, China;
4. Chinese National Engineering Research Centre for Control and Treatment of Heavy Metal Pollution, Central South University, Changsha 410083, China

Received 1 April 2019; accepted 10 November 2019

Abstract: The effects of photogenerated-hole scavengers (ascorbic acid, oxalic acid, humic acid and citric acid) on chalcopyrite bioleaching in the presence of visible light were studied using *Acidithiobacillus ferrooxidans* (*A. ferrooxidans*). Four sets of bioleaching experiments were performed: (1) visible light + 0 g/L scavenger, (2) visible light + 0.1 g/L of different scavenger (ascorbic acid, oxalic acid, humic acid and citric acid), (3) dark + 0.1 g/L of different scavenger (ascorbic acid, oxalic acid, humic acid and citric acid), and (4) dark + 0 g/L scavenger (control group). The results showed that ascorbic acid and oxalic acid could act as photogenerated-hole scavengers and significantly enhance chalcopyrite bioleaching under visible light. The dissolved copper in the light group without scavenger was only 18.7% higher than that of the control group. The copper extraction rates of the light groups with oxalic acid and ascorbic acid were respectively 30.1% and 32.5% higher than those of the control group. Scanning electron microscopy (SEM), X-ray diffraction (XRD) and Fourier transform infrared spectroscopy (FT-IR) analyses indicated that ascorbic acid and oxalic acid as photogenerated-hole scavenger could capture photo-generated holes and inhibit jarosite formation on the chalcopyrite surface, thereby enhancing bioleaching of chalcopyrite under visible light.
Key words: bioleaching; chalcopyrite; photogenerated-hole scavenger; visible light; *Acidithiobacillus ferrooxidans*

1 Introduction

As the most abundant copper sulfide mineral and primary copper resources, chalcopyrite has attracted extensive attention in copper extraction [1]. Until now, pyrometallurgy has been the main process for extracting copper from chalcopyrite [2]. However, these traditional processes have some shortcomings including high emission of polluted gas such as SO_2 and high cost [3]. Bioleaching (biohydrometallurgy) is a promising technology described as the microbe-assisted dissolution of sulfide ores, which provides a more environmentally friendly alternative to many traditional metal extraction methods, such as pyrometallurgy and conventional hydrometallurgy [4]. Up to now, nearly a quarter of the world's copper production is obtained through biohydrometallurgy [5]. However, commercial-scale chalcopyrite bioleaching has not

Foundation item: Project (41773089) supported by the National Natural Science Foundation of China; Project (2017SK2255) supported by the Key R&D Program of Hunan Province, China; Project (2015CNERC-CTHMP-05) supported by the Opening Foundation of the Chinese National Engineering Research Center for Control and Treatment of Heavy Metal Pollution, China; Project (CX20190136) supported by the Hunan Provincial Innovation Foundation for Postgraduates, China; Project (CSUZC201808) supported by the Open-End Fund for the Valuable and Precision Instruments of Central South University, China
Corresponding author: Jian-yu ZHU, Min GAN; Tel: +86-13755146512; E-mail: zhujy@csu.edu.cn, ganmin0803@sina.com
DOI: 10.1016/S1003-6326(19)65192-7

yet been fully developed due to its extremely slow kinetics and poor copper recovery [6]. To overcome these drawbacks, many researchers have exploited various methods for the enhancement of chalcopyrite bioleaching in recent decades, such as the adjustment of redox potentials and pH, adding "catalyst"-like activated carbon, silver ions and surfactant, and using mixed thermophilic bacteria [7−11]. These methods have promoted chalcopyrite bioleaching to some extent. However, these methods have neglected the semiconducting property of chalcopyrite during the bioleaching processes. In recent decades, semiconductor photocatalytic technology, such as photocatalytic degradation of organic pollutants, photocatalytic disinfection, photocatalytic reduction of carbon dioxide and photocatalytic generation of hydrogen, has been widely studied [12]. Some researchers have found that the visible light-excited photoelectrons from semiconductor minerals are capable of reducing ferric ions to ferrous ions, which can be used as an energy substrate for *Acidithiobacillus ferrooxidans* (*A. ferrooxidans* or *A. f.*) growth [13,14]. *A. ferrooxidans*, an acidophilic chemolithoautotrophic bacterium that obtains energy through oxidation of ferrous species and reduced sulfur compounds, is the most widely studied bioleaching bacterium due to its ability to extract metals, such as copper, zinc and gold [15,16]. Recent studies have shown that visible light can significantly accelerate copper dissolution due to the semiconductor property of chalcopyrite [17−19].

The bacteriostatic effect of photogenerated-holes and the rapid recombination of photo-generated electrons and holes (approximately 10 ns) in chalcopyrite particles limit the efficiency of photocatalytic chalcopyrite bioleaching [20,21]. Hence, capturing photogenerated-holes is the key issue for improving the photocatalytic efficiency of chalcopyrite bioleaching. Reductive organic compounds, such as ascorbic acid, humic acid, oxalic acid and citric acid are widespread in nature, and can serve as photogenerated-hole scavengers [22,23]. In addition, complexes formed by iron ions and the carboxyl groups of organic compounds have a strong photoreduction ability [24], which can enhance the utilization efficiency of photogenerated electron. However, to the best of our knowledge, no studies have reported the effect of organic compounds acting as photogenerated-hole scavengers on photocatalytic chalcopyrite bioleaching. In this work, the effect of photogenerated-hole scavengers on photocatalytic chalcopyrite bioleaching by *A. ferrooxidans* was investigated. X-ray diffraction (XRD), scanning electron microscopy (SEM) and Fourier transform infrared spectroscopy (FT-IR) were applied to monitoring changes on chalcopyrite surfaces to better understand the role of photogenerated-hole scavengers during chalcopyrite bioleaching under visible light.

2 Experimental

2.1 Strain and growth conditions

A. ferrooxidans strain ATCC 23270 was purchased from the American Type Culture Collection and used in this study. *A. ferrooxidans* was cultivated in 0K medium, which comprised 3 g/L $(NH_4)_2SO_4$, 0.1 g/L KCl, 0.5 g/L $K_2HPO_4\cdot 3H_2O$, 0.5 g/L $MgSO_4\cdot 7H_2O$ and 0.01 g/L $Ca(NO_3)_2$, and was adjusted to pH 2.0 with H_2SO_4 (0.01 mol/L). Chalcopyrite at 20 g/L was added to the 0K medium as an energy source. *A. ferrooxidans* was previously adapted in 0K medium containing 20 g/L chalcopyrite sample at 30 °C and 170 r/min. The cell number was quantified by hemocytometry using an optical microscope. Cells were harvested at the mid-logarithmic growth phase with cell concentrations greater than 1.0×10^7 cells/mL. The culture was first filtered through Whatman 42 filter paper to remove suspended solids. The filtrate containing cells was subsequently centrifuged at 25 °C for 20 min to obtain pellets containing bacteria. The pellets were washed with 0.01 mol/L sulfuric acid to obtain metabolite-free cells for further experiments.

2.2 Preparation of minerals

The chalcopyrite sample used in this work was purchased from Guilin Wantong Popular Science Museum of Natural Mineral Specimens, Guangxi, China. It was ground and sieved to obtain mineral powder with a particle size of 43−74 μm and then stored in a nitrogen atmosphere. The X-ray fluorescence spectral analysis indicated that the chalcopyrite ore contained 32.62% Cu, 29.82% Fe, 29.47% S, 5.29% O, 1.43% Si and 0.93% Ba. The XRD analysis showed that the main phase

compositions of the ore were chalcopyrite, jarosite and sulfur.

2.3 Bioleaching experiments

Bioleaching experiments were carried out in 250 mL flasks containing 100 mL sterilized 9K medium (pH=2) and 2 g chalcopyrite. The initial pH and inoculum concentration of the bioleaching system were 2.0 and 3.2×10^7 cells/mL, respectively. The flasks were incubated at 30 °C and 170 r/min in the illumination incubator (TS−2102GZ), where the light intensity was set to be 8500 or 0 lux. The effects of photogenerated-hole scavengers on bioleaching efficiency were explored by adding 100 μL of 4 g/L reductive organic compounds (ascorbic acid, oxalic acid, humic acid and citric acid) to the bioleaching system every day in the first 25 days. During chalcopyrite bioleaching, the pH and redox potentials were regularly monitored every three days. Samples (200 μL of solution) were taken regularly every three days to evaluate the concentration of cupric ions, total irons, ferrous ions and bacteria in the bioleaching system. Sterile distilled water was used to compensate for evaporative water loss, and an equal volume of sterile 0K medium (pH=2) was used to compensate for the losses caused by sampling analysis. All the bioleaching experiments were performed in duplicate to guarantee the reliability of the experimental results.

2.4 Analytical techniques

The concentrations of cupric ions and iron ions were determined by the BCO spectrophotometric and o-phenanthroline spectrophotometric methods, respectively [25] (the standard curve correlation coefficients R^2 were greater than 0.999). The pH and redox potential of the bioleaching solution were measured by pH meter (PHS−3C) and ORP meter (BPP−922), respectively. The surface characteristics and mineral composition of the original ore and bioleaching residues were detected by SEM, XRD and FT-IR.

3 Results and discussion

3.1 Effects of photogenerated-hole scavengers and visible light on chalcopyrite bioleaching

The effects of photogenerated hole scavengers and visible light on chalcopyrite bioleaching were investigated. As shown in Fig. 1, the dissolution of chalcopyrite increased rapidly during the first 6 days and then slowly, which might be related to the inhibition of passive film on chalcopyrite dissolution [26]. The copper concentration of the dark groups with scavengers and the light group with citric acid decreased in the later stage of the bioleaching. Organic acids have been reported to readily form complexes with copper [27]. Therefore, the decrease in copper concentration in the later stage of bioleaching with scavengers may be due to the chelation of organic substances on copper ions. The copper concentrations of the light illumination group with no scavenger, ascorbic acid, oxalic acid, humic acid and citric acid addition after 27 d were (1.46±0.03), (1.60± 0.03), (1.63±0.04), (1.42±0.04) and (0.98±0.05) g/L, respectively, while the corresponding dissolved copper concentrations in the dark system were (1.23±0.03), (1.06±0.04), (0.88±0.04), (1.17±0.04) and (1.05±0.03) g/L, respectively. The results showed that visible light accelerated the chalcopyrite dissolution, and scavengers including ascorbic acid and oxalic acid further enhanced the photocatalytic efficiency. The dissolved copper of the light control group without scavengers was 18.7% higher than that of dark control group without scavengers. Copper solubilization in the light group with ascorbic acid was 9.6% and 30.1% higher than that in the light and dark treatments without ascorbic acid, respectively. The dissolved copper in the light group with oxalic acid was 11.6% higher than that in the light group without scavengers and 32.5% higher than that in the dark group without scavengers. However, uniformly, the copper concentration in the dark group with scavengers was lower than that in the dark control group, which may be attributed to the complexation of organic compounds with copper ions. The promotion effect of ascorbic acid and oxalic acid was only achieved under light condition.

Total iron and ferrous iron concentration changes are plotted in Fig. 2. The variation trends in the total iron ion and ferrous ion concentration with different scavengers were generally consistent. Total iron increased rapidly initially accompanied by chalcopyrite dissolution followed by a decreasing trend. The decrease most likely can be attributed to jarosite formation, which further resulted in an inhibition effect. For ferrous ions, the

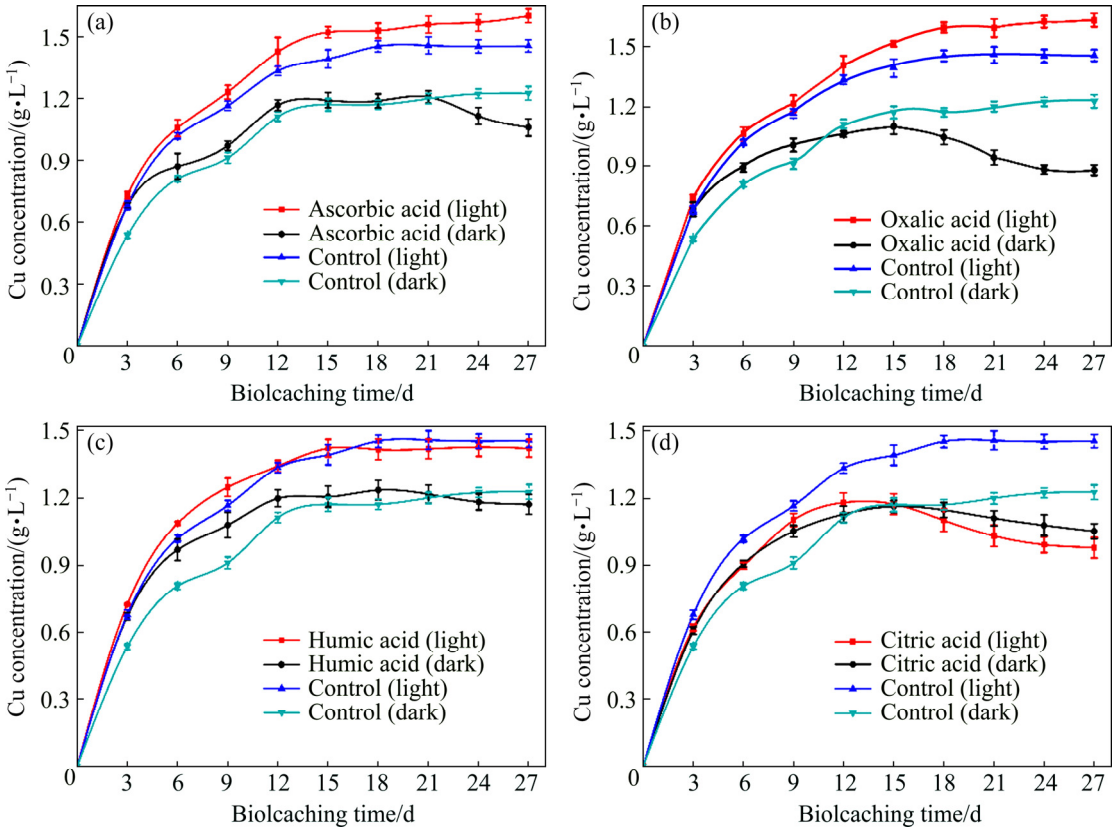

Fig. 1 Changes in concentration of dissolved copper during chalcopyrite bioleaching by different scavengers: (a) Ascorbic acid; (b) Oxalic acid; (c) Humic acid; (d) Citric acid

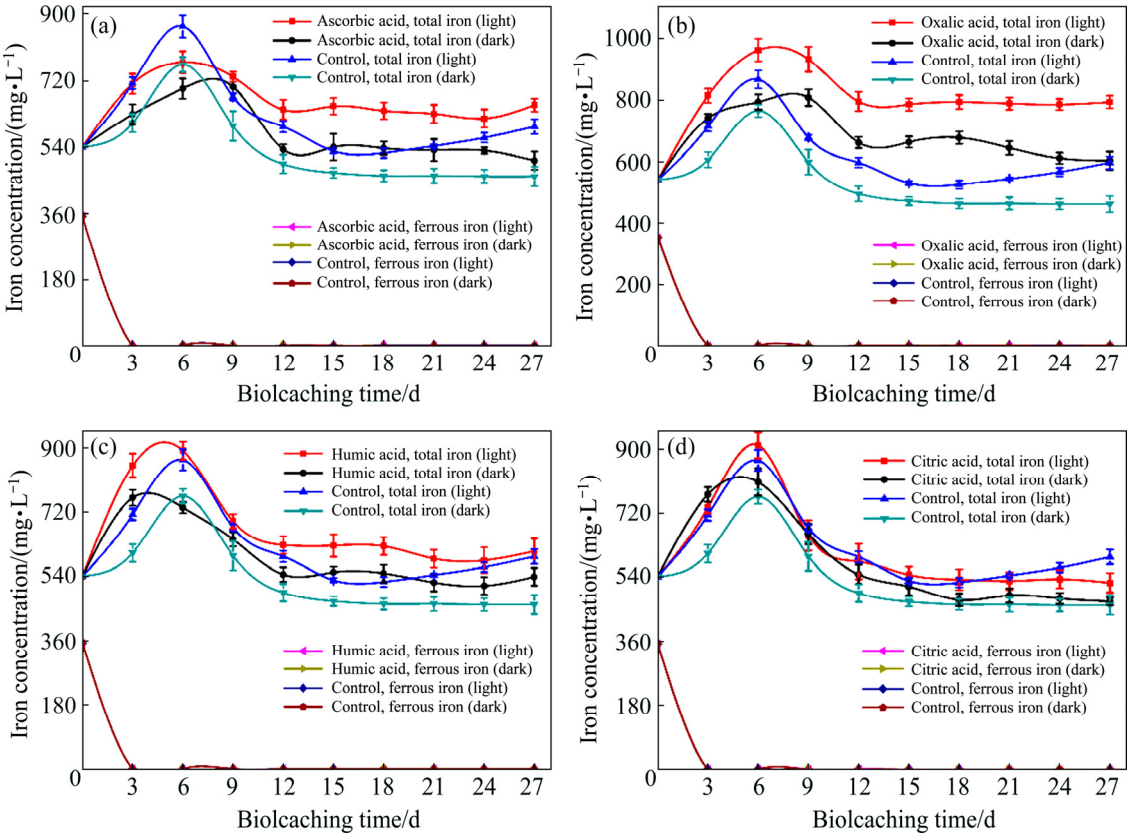

Fig. 2 Change in concentration of dissolved iron during chalcopyrite bioleaching by different scavengers: (a) Ascorbic acid; (b) Oxalic acid; (c) Humic acid; (d) Citric acid

concentration decreased rapidly in the first 3 days and was then maintained at a low level. This was due to the Fe(II) oxidization reaction caused by the rapid growth of bacteria. The photocatalytic reaction can be activated by visible light with energy equal to or greater than the band-gap energy [28], thereby generating electrons in the conduction band (CB) and holes in the valence band (VB) of the chalcopyrite. The photogenerated electrons can reduce Fe^{3+} to Fe^{2+}, giving rise to the regeneration of Fe^{2+} in the photocatalytic system [18]. As visible light can promote Fe^{3+}/Fe^{2+} cycling and Fe^{2+} regeneration, total iron and ferrous iron concentrations of the photocatalytic system were significantly higher than those of the dark system. The total iron concentration of ascorbic acid groups was higher than that of groups without ascorbic acid. In addition, the ferrous concentration in the ascorbic acid groups was slightly higher than that of the control groups without ascorbic acid. These results may be mainly due to the following two reasons. On one hand, the reductive ascorbic acid can capture the photogenerated holes [29] to suppress the bacteriostatic effect of photogenerated-holes and the recombination of photogenerated electrons and holes, thus enhancing photocatalytic efficiency. On the other hand, reductive ascorbic acid can reduce iron ions to regenerate ferrous ions. The main biochemical reactions during the bioleaching are listed as [30]

$$CuFeS_2+4Fe^{3+}\rightarrow Cu^{2+}+5Fe^{2+}+2S^0 \quad (1)$$

$$CuFeS_2+4H^++O_2\rightarrow Cu^{2+}+Fe^{2+}+2S^0+2H_2O \quad (2)$$

$$4Fe^{2+}+4H^++O_2\xrightarrow{A.f.}4Fe^{3+}+2H_2O \quad (3)$$

$$2S^0+3O_2+2H_2O\xrightarrow{A.f.}2SO_4^{2-}+4H^+ \quad (4)$$

$$K^++3Fe^{3+}+2SO_4^{2-}+6H_2O\rightarrow KFe_3(SO_4)_2(HO)_6+6H^+ \quad (5)$$

The presence of Fe^{3+} in the leaching solution has been widely accepted as the main factor for the indirect bioleaching mechanism of chalcopyrite (Eq. (1)) [31]. In addition, ferrous irons (Fe^{2+}) can be used as an energy source for *A. ferrooxidans*. Hence, the concentration of total iron is an important parameter in the bioleaching of chalcopyrite, and the high concentration of total iron should be beneficial for copper extraction. However, the copper concentration of the dark group with ascorbic acid did not increase compared with the dark group without ascorbic acid. This might be due to the bacteriostatic effect of organic compounds under the dark condition, which counteracted the effect of ascorbic acid on Fe^{2+} regeneration. These results indicated that ascorbic acid could capture photogenerated holes to suppress the bacteriostatic effects of photogenerated holes and the recombination of photogenerated electrons and holes, which could significantly enhance photocatalytic chalcopyrite bioleaching. The total iron concentration of groups with oxalic acid was significantly higher than that of groups without oxalic acid. The ferrous iron concentration of groups with oxalic acid was slightly higher than that of groups without oxalic acid. In addition, the total iron and ferrous iron concentrations of the light group with oxalic acid were higher than those of the dark group with oxalic acid because oxalic acid can capture photogenerated holes [23], which leads to a higher concentration of total iron and ferrous ion. In addition, the complexes formed by carboxyl groups and iron ions have a strong photoreduction ability [24], which also increases the concentration of iron ions and ferrous ions in the oxalic acid and ascorbic acid treatment systems. The effects of humic acid and citric acid on total iron and ferrous ion concentration in the leaching system were not obvious. This showed that humic acid and citric acid had little ability to capture photogenerated holes.

Figure 3 shows the change in concentration of *A. ferrooxidans* during chalcopyrite bioleaching with different photogenerated-hole scavengers. The concentration of bacteria increased slowly during the first 6 days of adaptation, then increased rapidly, reached maximum growth within 15 days, and finally maintained in a stable range. The bacterial growth of light groups was significantly higher than that of dark groups, which was due to the photogenerated electrons regenerating Fe^{2+} and promoting bacterial growth. Humic acid and citric acid had a slight inhibitory effect on the growth of *A. ferrooxidans*. Ascorbic acid and oxalic acid could slightly inhibit bacteria growth under the dark condition but promoted bacterial growth under the light condition. This might be due to the reaction of ascorbic acid and oxalic acid with photogenerated-holes, which suppressed the bacteriostatic effects of photogenerated holes and organic matter. Moreover, ascorbic acid and oxalic acid could effectively

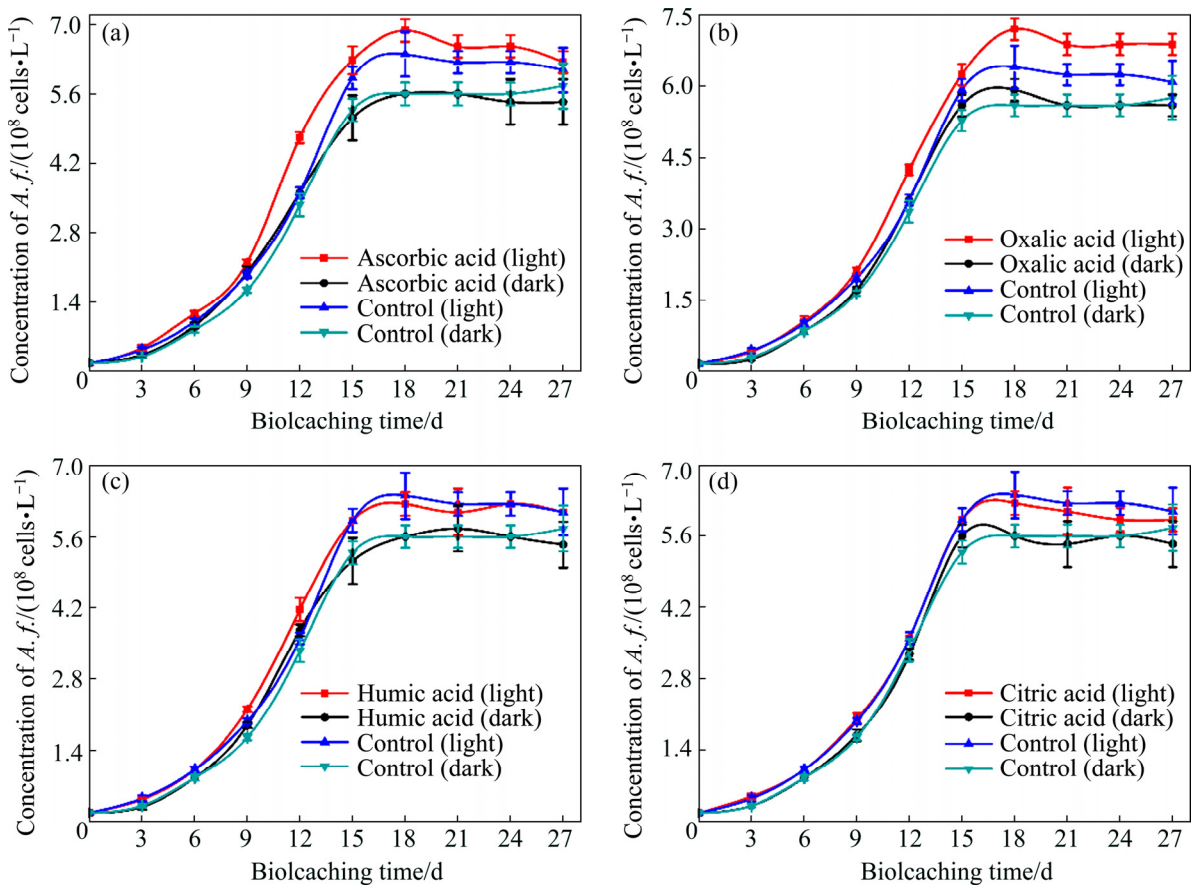

Fig. 3 Change in concentration of cells during chalcopyrite bioleaching by different scavengers: (a) Ascorbic acid; (b) Oxalic acid; (c) Humic acid; (d) Citric acid

reduce the recombination of photogenerated holes and electrons, and improve the utilization efficiency of the photogenerated electrons. These results are also consistent with the changes in copper ions and iron ions (Fig. 1 and Fig. 2).

The trends in pH change in the bioleaching system with different scavengers were essentially similar (shown in Fig. 4). The pH value of the bioleaching systems increased in the first 3 days and subsequently decreased rapidly to below 1.9. The initial increase in pH might be due to the fact that there was no available oxidizing agent in the early bioleaching system, and chalcopyrite dissolution consumed a large amount of H^+ (Eqs. (2) and (3)). The following drop in pH implied the generation of acids, which were produced by *A. ferrooxidans* oxidizing elemental sulfur to sulfuric acid and were the result of jarosite precipitation (Eqs. (4) and (5)). Compared with the dark groups, the more pronounced pH decrease in the light groups was a result of more acid generated by higher biomass and more jarosite formation, which was also consistent with the experimental results (shown in Fig. 3 and Table 1). The pH value of the light group with ascorbic acid was lower than that of the light group without ascorbic acid. The pH value of the dark group with ascorbic acid was not significantly different from that of the dark group without ascorbic acid. These were mainly due to the fact that ascorbic acid could effectively capture photogenerated-holes to suppress the bacteriostatic effect of photogenerated-holes and the recombination of photogenerated holes and electrons. The pH values of oxalic acid groups were lower than those of the control group without oxalic acid, because oxalic acid could capture photogenerated-holes and increase photocatalytic efficiency, thus promoting bacterial growth and producing more H^+. In addition, oxalic acid itself had strong acidity, resulting in a decrease in pH value in the bioleaching system. Humic acid and citric acid had little effect on the pH value of the bioleaching system due to their poor ability to scavenge photogenerated-holes.

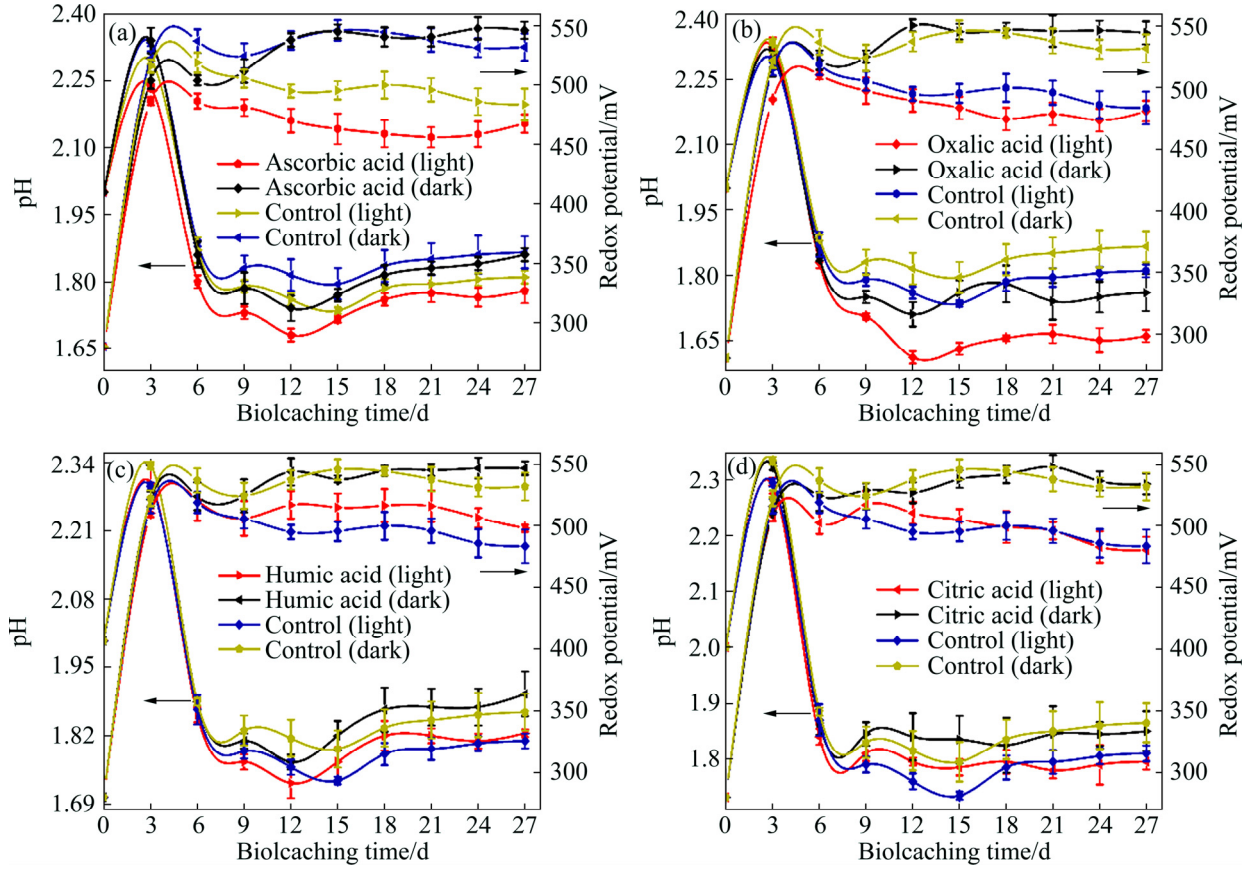

Fig. 4 pH and redox potential during chalcopyrite bioleaching by different scavengers: (a) Ascorbic acid; (b) Oxalic acid; (c) Humic acid; (d) Citric acid

The redox potential change trends of the different scavenger systems are shown in Fig. 4. The redox potential of each leaching system increased rapidly to above 480 mV in the first 3 days and then maintained in a relatively stable range. The redox potential of the light groups was lower than that of the dark groups, and the redox potential of the light groups with ascorbic acid or oxalic acid was lower than that of the light group without scavengers. The redox potential was partially related to the Fe^{3+}/Fe^{2+} ratio. The lower potential of the light groups was due to the regeneration of Fe^{2+} and continuous cycling of Fe^{3+}/Fe^{2+}, which was further induced by photocatalysis of the semiconducting chalcopyrite. The light groups with ascorbic acid or oxalic acid had a lower redox potential because ascorbic acid and oxalic acid could enhance photocatalytic efficiency. All in all, ascorbic acid and oxalic acid could enhance photocatalytic chalcopyrite bioleaching mainly by further accelerating the Fe^{3+}/Fe^{2+} cycling of the bioleaching system under light condition.

3.2 Surface morphology and composition analysis

The surface morphologies of the chalcopyrite before and after bioleaching were observed by SEM (Fig. 5). The surface morphology of the original chalcopyrite was smooth and clear, demonstrating that almost no passivation layer was attached to surface (Figs. 5(a_1, a_2)). Although chalcopyrite samples contained a small amount of jarosite, we did not observe jarosite by SEM because of its low content. The surfaces of chalcopyrite residues of groups without scavengers contained a large number of compact particles (Figs. 5(b_1, b_2, c_1, c_2)). According to the SEM−EDX analysis in Fig. 6, these compact particles contained potassium, iron, sulfur and oxygen, which are the main elements of jarosite. In addition, jarosite was reported to be cubic crystals with sizes ranging from 200 to 1000 nm [32], which is approximately the same as the morphology and size of the dense particles in our results. Based on the above, we speculate that these particles might be jarosite. The surface of residues of the ascorbic acid groups had almost no

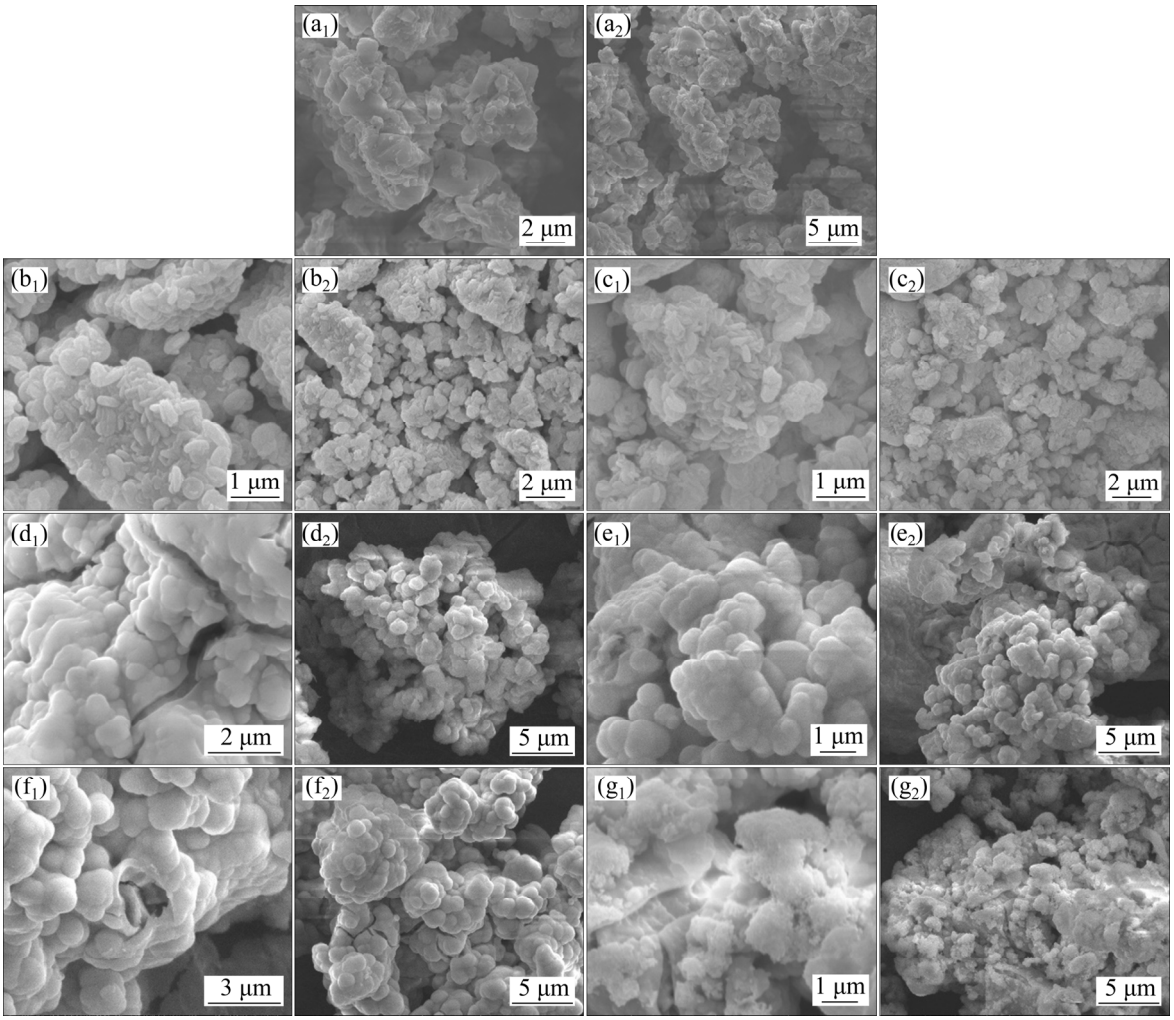

Fig. 5 SEM images of original chalcopyrite and chalcopyrite residues: (a_1, a_2) Original chalcopyrite surface; (b_1, b_2) Chalcopyrite residues surface without scavengers under light condition; (c_1, c_2) Chalcopyrite residues surface without scavengers under dark condition; (d_1, d_2) Chalcopyrite residues surface with ascorbic acid under light condition; (e_1, e_2) Chalcopyrite residues surface with ascorbic acid under dark condition; (f_1, f_2) Chalcopyrite residues surface with oxalic acid under light condition; (g_1, g_2) Chalcopyrite residues surface with oxalic acid under dark condition

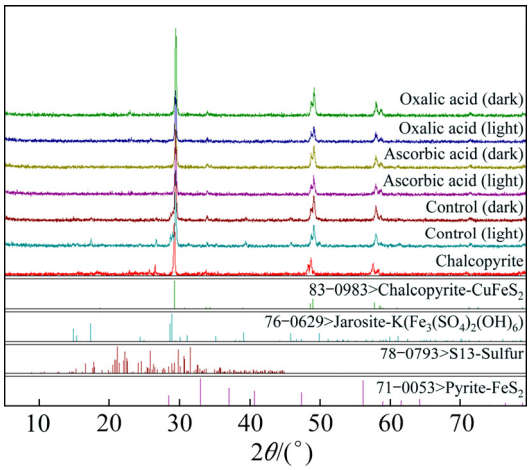

Fig. 6 XRD patterns of original chalcopyrite and chalcopyrite residues after bioleaching

jarosite but were covered with a large number of loose amorphous core−shell secondary iron mineral (Figs. 5(d_1, d_2, e_1, e_2)). The residues surface of oxalic acid group under light condition also contained a large number of core−shell secondary iron minerals (Figs. 5(f_1, f_2)), while the residues surface of the oxalic acid group under the dark condition had a large number of villous secondary iron mineral formation (Fig. 5(g_1, g_2)). These secondary iron minerals had a loose structure, which reduced the inhibitory effect of jarosite on chalcopyrite dissolution. The SEM results showed that ascorbic acid and oxalic acid could promote chalcopyrite bioleaching by forming a loose core−shell secondary iron mineral on the surface of the chalcopyrite.

The XRD phase retrieval analysis presented in Fig. 7 and Table 1 showed changes in the main phase composition of the chalcopyrite before and after bioleaching. The residues of the light group without scavengers contained more jarosite and less chalcopyrite than those of the corresponding dark group. However, ascorbic acid or oxalic acid added groups contained almost no jarosite. Additionally, a trace of elemental sulfur also existed in the residues. These results illustrated that most of the elemental sulfur was oxidized to sulfur oxides by *A. ferrooxidans* through the thiosulfate pathway (Eq. (4)) [30]. It was confirmed that jarosite was the most abundant product continuously accumulated during the bioleaching of chalcopyrite [33]. The passivation effect in bioleaching was mainly derived from the jarosite on the chalcopyrite surface. Visible light could enhance chalcopyrite bioleaching, which also resulted in more jarosite formation and inhibited further dissolution of chalcopyrite. Ascorbic acid and oxalic acid could reduce jarosite formation, thus further promoting chalcopyrite bioleaching. This was also consistent with the SEM analysis results. These results suggested that ascorbic acid and oxalic acid groups could form loose secondary iron mineral to reduce the formation of jarosite.

FT-IR spectra presented in Fig. 8 showed changes in the surface groups of chalcopyrite before and after bioleaching. The intense adsorption peaks observed at 3332−3433 and 1631 cm^{-1} corresponded to the hydroxyl and H_2O group of the jarosite, respectively [34]. Three peaks appeared near 1200, 1080 and 1000 cm^{-1}, which were assigned to the S—O bending vibration in jarosite [35]. The characteristic peaks of jarosite containing S—O bending vibration, hydroxyl and H_2O groups appeared in the original chalcopyrite and the chalcopyrite residues without scavengers. The characteristic jarosite peaks of the dark group without scavengers were obviously stronger than

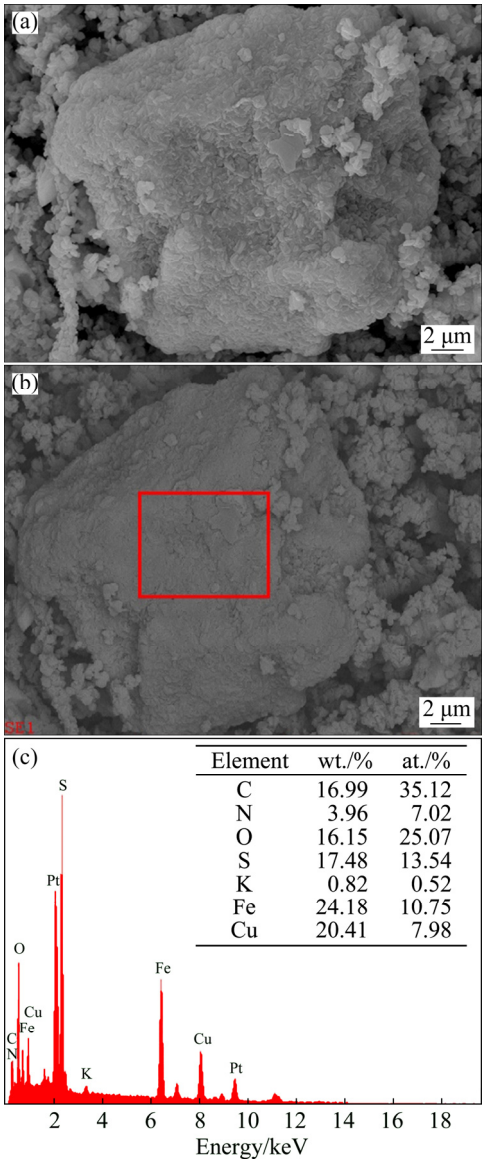

Fig. 7 SEM−EDS analysis results of chalcopyrite after bioleaching without scavenger

Table 1 Analysis results of ore residues and original ore by XRD

Organic matter	Light condition	Time/d	Content in residue/%			
			Chalcopyrite	Jarosite	Sulfur	Pyrite
−	−	0	91.2	5.6	2.7	0.5
−	8500 lux	36	69.1	29.4	1.3	0.2
−	Dark	36	80.5	17.6	1.4	0.5
Ascorbic acid	8500 lux	36	92.4	0.7	5.1	1.8
Ascorbic acid	Dark	36	92.1	0.8	5.8	1.3
Oxalic acid	8500 lux	36	90.9	2.1	6.9	0.1
Oxalic acid	Dark	36	98.8	0.8	0.3	0.1

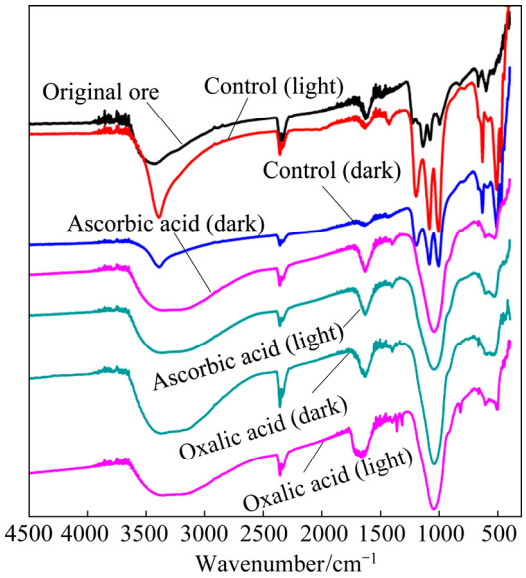

Fig. 8 FT-IR spectra of original chalcopyrite and chalcopyrite residues after bioleaching for 27 days

those of the original chalcopyrite. The characteristic jarosite peaks of the light group without scavengers were obviously stronger than those of the corresponding dark group and original chalcopyrite. These observations indicated that a large amount of jarosites formed during chalcopyrite bioleaching, especially in the light group without scavengers. However, the residues treated with ascorbic acid and oxalic acid had no characteristic peaks for jarosite, but another new peak appeared near 1045 cm^{-1}. This new peak was caused by the C—O stretching vibration [36]. This result illustrated that chalcopyrite bioleaching with ascorbic acid and oxalic acid formed other new substances to replace jarosite formation during the bioleaching in accordance with the results of the SEM and XRD analyses. These results suggested that visible light could promote chalcopyrite bioleaching, resulting in more jarosite formation, while ascorbic acid and oxalic acid could form a loose amorphous core−shell secondary iron mineral to inhibit jarosite formation on the chalcopyrite surface, further enhancing photocatalytic chalcopyrite bioleaching.

Based on the analysis above, the mechanism of scavenger promoting photocatalytic chalcopyrite bioleaching is summarized in Fig. 9. Ascorbic acid and oxalic acid as photogenerated-hole scavenger could capture photo-generated holes and inhibit jarosite formation on the chalcopyrite surface, thereby enhancing bioleaching of chalcopyrite under visible light.

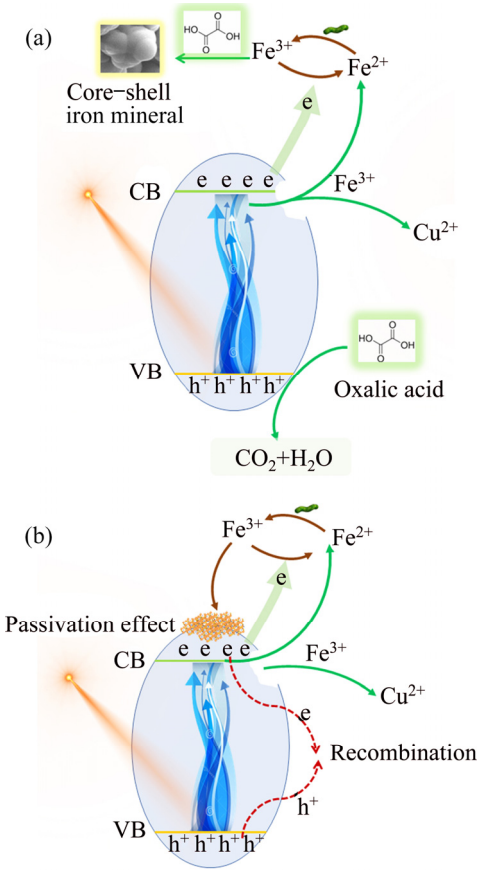

Fig. 9 Mechanism of scavengers promoting photo-catalytic chalcopyrite bioleaching: (a) Addition of photogenerated-holes scavenger; (b) Without addition of photogenerated-holes scavenger

4 Conclusions

(1) Ascorbic acid and oxalic acid can significantly enhance the photocatalytic efficiency of chalcopyrite bioleaching. The dissolved copper in the light group without scavengers was only 18.7% higher than that of the corresponding dark group. The copper extraction rate of the light group with ascorbic acid was 30.1% higher than that of the control group. The dissolved copper in the light group with oxalic acid was 32.5% higher than that of the control group.

(2) Ascorbic acid and oxalic acid can suppress the bacteriostatic effect of photogenerated-holes and the recombination of photogenerated holes and electrons through capturing photogenerated-holes, thus enhancing the photocatalytic efficiency of chalcopyrite bioleaching.

(3) Ascorbic acid and oxalic acid can also inhibit jarosite formation on the chalcopyrite surface by forming a loose amorphous core−shell

secondary iron mineral, thus promoting photocatalytic chalcopyrite bioleaching.

References

[1] LIU H C, XIA J L, NIE Z Y, WEN W, YANG Y, MA C Y, ZHENG L, ZHAO Y D. Formation and evolution of secondary minerals during bioleaching of chalcopyrite by thermoacidophilic Archaea *Acidianus manzaensis* [J]. Transactions of Nonferrous Metals Society of China, 2016, 26: 2485−2494.

[2] CÓRDOBA E M, MUÑOZ J A, BLÁZQUEZ M L, GONZÁLEZ F, BALLESTER A. Leaching of chalcopyrite with ferric ion. Part I: General aspects [J]. Hydrometallurgy, 2008, 93: 81−87.

[3] DIMITRIJEVIĆ M, KOSTOV A, TASIĆ V, MILOSEVIĆ N. Influence of pyrometallurgical copper production on the environment [J]. Journal of Hazardous Materials, 2009, 164: 892−899.

[4] ZHANG R Y, NEU T R, BLANCHARD V, VERA M, SAND W. Biofilm dynamics and EPS production of a thermoacidophilic bioleaching archaeon [J]. New Biotechnology, 2019, 51: 21−30.

[5] CASTRO C, DONATI E R. Improving zinc recovery by thermoacidophilic archaeon *Acidianus copahuensis* using tetrathionate [J]. Transactions of Nonferrous Metals Society of China, 2016, 26: 3004−3014.

[6] FENG S, YANG H, WANG W. Improved chalcopyrite bioleaching by *Acidithiobacillus* sp. via direct step-wise regulation of microbial community structure [J]. Bioresource Technology, 2015, 192: 75−82.

[7] DAVIS-BELMAR C, GALLARDO I, DEMERGASSO C, RAUTENBACH G. Effect of organic extractant LIX 84IC, pH and temperature changes on bioleaching microorganisms during SX treatment [J]. Hydrometallurgy, 2012, 129: 135−139.

[8] ZHAO H, WANG J, YANG C, HU M, GAN X, TAO L, QIN W, QIU G. Effect of redox potential on bioleaching of chalcopyrite by moderately thermophilic bacteria: An emphasis on solution compositions [J]. Hydrometallurgy, 2015, 151: 141−150.

[9] MA Y L, LIU H C, XIA J L, NIE Z Y, ZHU H R, ZHAO Y D, CHEN-YAN M A, ZHENG L, HONG C H, WEN W. Relatedness between catalytic effect of activated carbon and passivation phenomenon during chalcopyrite bioleaching by mixed thermophilic Archaea culture at 65 °C [J]. Transactions of Nonferrous Metals Society of China, 2017, 27: 1374−1384.

[10] LIU W, ZHANG S J, SUN F, LIU C. Catalytic effect of a combined silver and surfactant catalyst on cobalt ore bioleaching [J]. JOM, 2018, 70: 2819−2824.

[11] HAO X D, LIU X D, YANG Q, LIU H W, YIN H Q, QIU G Z, LIANG Y L. Comparative study on bioleaching of two different types of low-grade copper tailings by mixed moderate thermophiles [J]. Transactions of Nonferrous Metals Society of China, 2018, 28: 1847−1853.

[12] GE J, ZHANG Y, PARK S J. Recent advances in carbonaceous photocatalysts with enhanced photocatalytic performances: A mini review [J]. Materials, 2019, 12: 1916.

[13] LU A, LI Y, JIN S, WANG X, WU X L, ZENG C, DING H, HAO R, LV M, WANG C. Growth of non-phototrophic microorganisms using solar energy through mineral photocatalysis [J]. Nature Communications, 2012, 3: 768.

[14] LU A, LI Y, JIN S. Interactions between semiconducting minerals and bacteria under light [J]. Elements, 2012, 8: 125−130.

[15] ZHU J, GAN M, ZHANG D, HU Y, CHAI L. The nature of *Schwertmannite* and *Jarosite* mediated by two strains of *Acidithiobacillus ferrooxidans* with different ferrous oxidation ability [J]. Materials Science and Engineering C, 2013, 33: 2679−2685.

[16] ZHANG X, FENG Y L, LI H R. Enhancement of bio-oxidation of refractory arsenopyritic gold ore by adding pyrolusite in bioleaching system [J]. Transactions of Nonferrous Metals Society of China, 2016, 26: 2479−2484.

[17] YANG B, LIN M, FANG J, ZHANG R, LUO W, WANG X, LIAO R, WU B, WANG J, GAN M, LIU B, ZHANG Y, LIU X, QIN W, QIU G. Combined effects of jarosite and visible light on chalcopyrite dissolution mediated by *Acidithiobacillus ferrooxidans* [J]. Science of the Total Environment, 2020, 698: 134175.

[18] ZHOU S, GAN M, ZHU J, LI Q, JIE S, YANG B, LIU X. Catalytic effect of light illumination on bioleaching of chalcopyrite [J]. Bioresource Technology, 2015, 182: 345−352.

[19] YANG B, GAN M, LUO W, ZHOU S, LEI P, ZENG J, SUN W, ZHU J, HU Y. Synergistic catalytic effects of visible light and graphene on bioleaching of chalcopyrite [J]. RSC Advances, 2017, 7: 49838−49848.

[20] BASSAID S, ROBERT D, CHAIB M. Use of oxalate sacrificial compounds to improve the photocatalytic performance of titanium dioxide [J]. Applied Catalysis B: Environmental, 2009, 86: 93−97.

[21] CUI Y, DU H, WEN L. Enhancement of photoelectrocatalytic properties of stainless-steel/TiO_2 electrode by applying mid- frequency electric field [J]. Environmental Chemistry Letters, 2009, 7: 321−324.

[22] BEMS B, JENTOFT F C, SCHLÖGL R. Photoinduced decomposition of nitrate in drinking water in the presence of titania and humic acids [J]. Applied Catalysis B: Environmental, 1999, 20: 155−163.

[23] KRETSCHMER I, SENN A M, MEICHTRY J M, CUSTO G, HALAC E B, DILLERT R, BAHNEMANN D W, LITTER M I. Photocatalytic reduction of Cr(VI) on hematite nanoparticles in the presence of oxalate and citrate [J]. Applied Catalysis B: Environmental, 2019, 242: 218−226.

[24] REN H T, JI Z Y, WU S H, HAN X, LIU Z M, JIA S Y. Photoreductive dissolution of schwertmannite induced by oxalate and the mobilization of adsorbed As(V) [J]. Chemosphere, 2018, 208: 294−302.

[25] MA L, WANG X, FENG X, LIANG Y, XIAO Y, HAO X, YIN H, LIU H, LIU X. Co-culture microorganisms with different initial proportions reveal the mechanism of

chalcopyrite bioleaching coupling with microbial community succession [J]. Bioresource Technology, 2016, 223: 121−130.

[26] QIN W, YANG C, LAI S, WANG J, LIU K, ZHANG B. Bioleaching of chalcopyrite by moderately thermophilic microorganisms [J]. Bioresource Technology, 2013, 129: 200−208.

[27] INABA S, TAKENAKA C. Effects of dissolved organic matter on toxicity and bioavailability of copper for lettuce sprouts [J]. Environment International, 2005, 31: 603−608.

[28] BARAKAT M, SCHAEFFER H, HAYES G, ISMAT-SHAH S. Photocatalytic degradation of 2-chlorophenol by Co-doped TiO_2 nanoparticles [J]. Applied Catalysis B: Environmental, 2005, 57: 23−30.

[29] PERAL J, MILLS A. Factors affecting the kinetics of methyl orange reduction photosensitized by colloidal CdS [J]. Journal of Photochemistry and Photobiology A: Chemistry, 1993, 73: 47−52.

[30] FENG S, YANG H, WANG W. Insights to the effects of free cells on community structure of attached cells and chalcopyrite bioleaching during different stages [J]. Bioresource Technology, 2016, 200: 186−193.

[31] GOVENDER-OPITZ E, KOTSIOPOULOS A, BRYAN C G, HARRISON S T L. Modelling microbial transport in simulated low-grade heap bioleaching systems: The hydrodynamic dispersion model [J]. Chemical Engineering Science, 2017, 172: 545−558.

[32] YU R, SHI L, GU G, ZHOU D, YOU L, CHEN M, QIU G, ZENG W. The shift of microbial community under the adjustment of initial and processing pH during bioleaching of chalcopyrite concentrate by moderate thermophiles [J]. Bioresource Technology, 2014, 162: 300−307.

[33] PRADHAN N, NATHSARMA K, RAO K S, SUKLA L, MISHRA B. Heap bioleaching of chalcopyrite: A review [J]. Minerals Engineering, 2008, 21: 355−365.

[34] GUNNERIUSSON L, SANDSTRÖM Å, HOLMGREN A, KUZMANN E, KOVACS K, VÉRTES A. Jarosite inclusion of fluoride and its potential significance to bioleaching of sulphide minerals [J]. Hydrometallurgy, 2009, 96: 108−116.

[35] LIANG C L, XIA J L, ZHAO X J, YANG Y, GONG S Q, NIE Z Y, MA C Y, ZHENG L, ZHAO Y D, QIU G Z. Effect of activated carbon on chalcopyrite bioleaching with extreme thermophile *Acidianus manzaensis* [J]. Hydrometallurgy, 2010, 105: 179−185.

[36] PAL S, JOY S, KUMBHAR P, TRIMUKHE K D, VARMA A J, PADMANABHAN S. Effect of mixed acid catalysis on pretreatment and enzymatic digestibility of sugar cane bagasse [J]. Energy & Fuels, 2016, 30: 7310−7318.

利用光生空穴清除剂强化光催化黄铜矿生物浸出

杨宝军[1,2]，罗 雯[3]，廖 骐[4]，朱建裕[1,2,4]，甘 敏[1,2]，刘学端[1,2]，邱冠周[1,2]

1. 中南大学 资源加工与生物工程学院，长沙 410083；
2. 中南大学 生物冶金教育部重点实验室，长沙 410083；
3. 中南大学 湘雅二医院，长沙 410011；
4. 中南大学 国家重金属污染防治工程技术研究中心，长沙 410083

摘 要：通过嗜酸氧化亚铁硫杆菌(*Acidithiobacillus ferrooxidans*)研究光生空穴清除剂(抗坏血酸、草酸、腐质酸和柠檬酸)对光催化黄铜矿生物浸出的影响。设置 4 组生物浸出实验：(1)可见光 + 0 g/L 光生空穴清除剂；(2)可见光 + 0.1 g/L 不同光生空穴清除剂(抗坏血酸、草酸、腐植酸和柠檬酸)；(3)黑暗 + 0.1 g/L 不同光生空穴清除剂(抗坏血酸、草酸、腐植酸和柠檬酸)；(4)黑暗 + 0 g/L 光生空穴清除剂(对照组)。结果表明，光照条件下，抗坏血酸和草酸作为光生空穴清除剂时，能够显著促进黄铜矿生物浸出。可见光 + 0 g/L 光生空穴清除剂组的铜离子溶出率比对照组高 18.7%；可见光 + 0.1 g/L 草酸组和可见光 + 0.1 g/L 抗坏血酸组的黄铜矿溶出率分别比对照组高 30.1%和 32.5%。SEM，XRD 和 FT-IR 分析表明，抗坏血酸和草酸作为光生空穴清除剂能够捕获光生空穴和抑制黄钾铁矾在黄铜矿表面形成，从而促进光催化黄铜矿的生物浸出。

关键词：生物浸出；黄铜矿；光生空穴清除剂；可见光；嗜酸氧化亚铁硫杆菌

(Edited by Bing YANG)